Desalination and Water Treatment
www.deswater.com

doi: 10.5004/dwt.2019.24049

155 (2019) 272–284
July

Effective removal of Pb^{2+} and Cu^{2+} from highly concentrated aqueous solutions: comparative sorption study

T.N. Myasoedova[a,*], Yu.S. Miroshnichenko[a], V.A. Gadzhieva[a], A.I. Chechevatov[b], M.A. Kremennaya[b], Yu.V. Popov[c], G.I. Lazorenko[d]

[a]*Southern Federal University, Institute of Nanotechnologies, Electronics and Equipment Engineering, Chekhov str. 2, Taganrog, 347928, Russia, email: tnmyasoedova@sfedu.ru (T.N. Myasoedova)*
[b]*Southern Federal University, Faculty of Physics, Zorge str. 5, Rostov-on-Don, 344090, Russia*
[c]*Southern Federal University, Institute of Earth Sciences, Zorge str. 40, Rostov-on-Don, 344090, Russia*
[d]*Rostov State Transport University, sq. Rostovskogo Strelkovogo Polka Narodnogo Opolchenia 2, Rostov-on-Don, 344038, Russia*

Received 12 November 2018; Accepted 1 March 2019

ABSTRACT

The study explored the sorption behavior of Cu^{2+} and Pb^{2+} ions onto humates obtained from brown coal wastes. The composition and structure of soluble and insoluble humates are analyzed by methods of SEM, EDX, and FTIR. SEM and EDX showed the multiphase structure of both humate samples, which changes significantly because of the sorption of heavy metals. It is observed that copper and lead are built in different ways into the humic matrix: The analysis of FTIR spectra revealed that sorption of Cu^{2+} ions of both samples is assumed to occur through formation of copper dycarbonyl ($Cu(CO)_2$) and ion-exchange mechanism, while in the case of lead sorption, phenolic and carboxyl groups are involved in the sorption process. The effect of various operational parameters such as pH, contact time, initial metal ions concentration and humates dose was investigated. The optimum pH for effective metal ion binding was found to be about 5.4–5.6 and 6.2–7.2, for Cu^{2+} and Pb^{2+} solutions, respectively. The optimum contact time was 1 h. The experimental results showed that both types of humates investigated in the work bind Pb^{2+} ions better than Cu^{2+} ones. H-B samples revealed the sorption capacity of 122 and 388 mg g^{-1} and H-GK samples of 58 and 350 mg g^{-1} for Cu^{2+} and Pb^{2+} ions, respectively. It was observed that HCl, HNO_3, H_2SO_4 acids are good eluents for H-B and H-GK regeneration (desorption reaches 100%). The kinetic studies revealed that sorption could be described by a pseudo-second-order rate equation. Thermodynamic studies showed that the values of $\Delta G°$ were negative at all temperatures confirming the feasibility of the sorption process. The positive value of $\Delta S°$ indicated that ion exchange reactions occurred.

Keywords: Humates; Copper ions; Lead ions; Sorption; Removal efficiency

1. Introduction

Heavy metals are well-known pollutants in both water and soil environments. To a large extent, their presence comes from industrial wastewater [1–4]. The discharge of sewage containing high concentrations of heavy metals in host reservoirs has serious adverse environmental consequences. The presence in water such metals as copper, lead, zinc, nickel, mercury, cadmium, chromium poses a significant threat to public health due to their resistance, biomagnification, and accumulation in the food chain. Severe effects include reduced growth and development, cancer, organ damage, nervous system damage. Therefore, the problem of wastewater treatment for industrial and drinking purposes is becoming more important from year to year.

* Corresponding author.

Industrial and domestic wastewater can contain copper up to 2,051.26 mg kg^{-1} and lead up to 93.73 mg kg^{-1} in their sludge [5]. The concentration of copper in wastewater above 1.9 mg kg^{-1} inhibits the digestion of precipitation in sewage treatment plants, 1.0 mg kg^{-1} reduces the effective purity by 5%, and 75 mg kg^{-1} is a volley discharge of metal and represents a danger to the equipment of treatment facilities.

To remove dissolved heavy metals ions from various environments, conventional techniques including chemical precipitation [6], ion exchange [7], reverse osmosis [8], membrane separation [9], electrochemical treatments [10], solvent extraction processes [11], and adsorption [12–15] are widely used. The simplest in hardware design, low cost, performing deep water purification is sorption method. Other advantages of this method are the high efficiency, possibility of cleaning from several substances simultaneously and recuperation of them. Application of sorbents allows to clean wastewaters without secondary pollution and to provide reliability in fluctuating volumes and composition of wastewater [16–17].

In recent years, interest is given to a new technique of purification from heavy metals based on the humic substances using as natural sorbents [18]. Humic substances are a mixture of complex organic compounds [19–21]. The sorbents can be manufactured from humic substances of brown coal wastes [22], peat and sapropel [20,23] by alkali extraction in ammonia, potassium hydroxide or sodium hydroxide solutions. Such treatment converts them into water-soluble salts - potassium or sodium humate possessing high chemical activity. An alternative way involves the mechanical crushing of brown coal with a solid alkali, resulting in solid potassium and sodium humate [3] A huge number of works are devoted to the usage of humic substances as sorbents for the detoxification of soil [20,24–26]. At the same time, not many studies are devoted to water purification with humic substances, especially the wastewater, containing high concentrations of heavy metals. In the work [27] the effective removal of Pb^{2+} in the aqueous solutions by adsorption onto insolubilized humic acid was investigated. The possibility of using sodium humate as a sorbent for water purification from Co^{2+} and Ni^{2+} was studied [3]. Humates form stable complexes with radionuclides, polyaromatic hydrocarbons, pesticides, chlorinated hydrocarbons, petroleum products [20], phenols, mineral oils, heavy metals [28–29], phosphorus [30] in water.

It is difficult to explain the interactions between humic substances and metal ions due to their heterogeneous, polyelectrolyte, and polydisperse nature. So, metal ions can bond with humic substances in following ways: (1) the purely electrostatic, nonspecific interaction; (2) the specific interactions leading to the formation of complexes and chelates with functional groups [30–37]. Carboxyl and hydroxyl groups play a key role in interaction processes. It is known that the binding of metals to humic acids/ humic acid salts depends on their type. Therefore, the key task is studying the mechanism of sorption and searching for optimal conditions of the sorption process [27,35,38,39]. The metal ion sorption capacity depends on the origin of humic substances and their pretreatment.

In our previous work [40] we showed the potential possibility of using humates, obtained from brown coal wastes (Irkutsk, Russia) as heavy metal sorbents.

This work follows our previous study and is focused mainly on the investigation of removal efficiency of copper(II) and lead(II) ions by two types of humates (soluble and insoluble) vs. different factors: pH, temperature, metal ion concentration, a dose of humate. The attempts to study the sorption ability of humates obtained from brown coal wastes to Cu^{2+} and Pb^{2+} from highly concentrated aqueous solutions in accordance with composition and structure were investigated to clarify the mechanisms of sorption. Kinetic and thermodynamic studies of metal ion sorption on humates are presented in the article. For the first time, studies were carried out on the regeneration of humate-based sorbents by different acids.

2. Materials and methods

2.1. Characterization of sorbents

The humates obtained from brown coal wastes were used in the experiment. There were two types of commercial humate samples: "Humat Baikal (matched as H-B), and "Humat – GK" (matched as H-GK) used as fertilizer agents for agriculture in USA, New Zealand, Australia, and Russia, Humate "H-B" - contains water-soluble salts- sodium humates, the solubility is not less than 92%. Humate "GK"- humic acid content not less than 82%, slightly soluble in water.

2.2. Chemicals and reagents

All chemicals used in this work were of analytical grade. Copper(II) sulfate, lead(II) nitrate, formic acid were purchased from Aquatest (Russia). The pH was adjusted by sulphuric acid and nitric acid also obtained from Aquatest.

2.3. Sorption/desorption experiments

Sorption was carried out in static conditions that lead to the formation of strong coordination compounds. To investigate the sorption capacity of humates, a series of Cu^{2+} and Pb^{2+} solutions with different concentrations (300–900 mg L^{-1}) were kept in contact with different amounts of H-B and H-GK samples (200–4,600 mg L^{-1}). Sorption experiments were done at pH 2 and pH that is reached after sorbent introduction (it is varied from 5.4 to 7.2 and depends on the type and dose of sorbent).

First, H-B and H-GK samples were added to the metal-containing solutions. The suspension was magnetically stirred at room temperature for 15 min and then left for some time (from 0.5 to 4 h) to saturate with the metal ion. Resulting suspensions were centrifuged and the supernatant liquor carefully was drawn off and analyzed for Cu^{2+} or Pb^{2+} content by potentiometer method. Solid H-B-Cu^{2+} and H-GK-Cu^{2+} complexes were dried and analyzed by FTIR.

The percentage removal of copper and lead ions was calculated with the following equation:

$$\%\text{Removal} = \frac{C_0 - C_e}{C_0} \times 100\% \quad (1)$$

where C_o is the initial metal ion concentration in the solution (mg L^{-1}); C_e is the equilibrium metal ion concentration in the solution (mg L^{-1}).

The regeneration of the H-B and H-GK sorbents was examined by acid treatment. The elution of Pb^{2+} and Cu^{2+} from H-B and H-GK was studied under batch conditions. First, the sorbents were contacted to Pb^{2+} and Cu^{2+} solutions as in sorption experiments. The initial metal ion concentration was 300 mg L^{-1}. The saturated H-B and H-GK samples were separated by centrifugation and washed with D.I. water. Thereafter, the centrifuged sorbents were treated with 50 mL 0.01 M acids: HCl, HNO_3, and H_2SO_4. The percentage of desorbed Pb^{2+} or Cu^{2+} was determined as:

$$\text{Desorption}\,(\%) = \frac{\text{Concentration of metal ion desorbed by acid}}{\text{Concentration of metal ion sorbed on H – B or H – GK}} \times 100\% \quad (2)$$

2.4. Instrumentation

Potentiometer (Ekotest-VA, Russia) was used to analyze Cu^{2+} and Pb^{2+} concentration in the solution. The hydrogen ion concentration in different solutions was measured by means of pH-meter (Ekotest-2000, Russia). The demanded dose of humates and other reagents were weighted on the analytical balance produced by VIBRA HT 84CE.

Both chemical composition and surface morphology investigations were carried out using complex analytic device based on scanning electron microscope VEGA II LMU with operating voltage at 20 kV and system of the microanalysis INCA ENERGY 450/XT with X-Act DDD detector and energy dispersive X-ray (EDX) analyzer (Oxford Instruments). The composition data was normalized to 100% and doesn't include carbon and water (semi-quantitative analysis). The detection limit of elements for EDX analysis is 0.1–0.5 wt%. To obtain images, the BSE detector is used (shows a phase contrast: different shades correspond to regions with different average atomic weight). The penetration depth of the signal was about 1 μm.

Thermogravimetric curves were obtained with samples of around 9 mg of the solid on the STA 449 F5 Jupiter from NETZSCH thermogravimetric analyzer in a dynamic atmosphere, using a dry nitrogen flux, with heating from room temperature up to 650°C at a heating rate of 4.3°C s^{-1}.

IR spectral analysis was performed on an ALPHA IR Fourier spectrometer (Bruker Optik GmbH, Germany) by the method of frustrated total internal reflection with the following parameters: resolution of 2 cm^{-1} and spectrum recording time of 50 scans. Spectra were recorded in the mid-IR range from 500 to 4,000 cm^{-1} using the OPUS software.

3. Results and discussion

3.1. SEM and chemical analysis

The morphology of the surfaces and micro elemental composition of H-GK and H-B humate samples were determined by the energy dispersive X-ray analysis (EDX) by simultaneously scanning electron microscope (SEM). Fig. 1 shows an image of H-GK and H-B humate samples before and after the sorption of Cu^{2+} and Pb^{2+}.

SEM images revealed the multiphase structure in both H-GK and H-B humate samples. Differences in the morphology of the initial humates are clearly visible. While H-GK has a hard, monolithic structure throughout the sample (Fig. 1(a)), H-B is formed by the mixing of friable, needle-shaped structures with rare and hard particles (Fig. 1(d)). In addition, there are significant changes in the morphology of humates after the sorption of Cu^{2+} and Pb^{2+}. Thus, both H-GK and H-B samples have a highly compacted monolithic structure, especially in the case of lead sorption (Figs. 1(c) and (f)). Copper forms aggregates in the structure of humates: small in H-B and larger in H-GK. In the case of lead, phase inclusions are not revealed. Lead is scattered in a humid matrix, and films relatively lead-enriched are observed on the surface and in the chips of the samples.

The humate composition of any one humic substance is specific for that substance. Thus there exists a large variability in the elemental composition of different humic substances. Humates from different mineral deposits would be expected to have their own unique features. In addition, each humate is characterized by a variety of phase composition that clearly affects their sorption ability. To illustrate the differences in the elemental composition of various humate regions (Fig.1, marked by dots), elemental analysis was carried out, the results of which are given in Tables 1 and 2 (labeled as "point"). Elemental analysis was carried out for all phases of humate constituents. The ranges of detected concentrations of elements and their mean values are presented in Tables 1 and 2.

From the analysis of Tables 1 and 2 it follows that both types of humates have approximately the same elemental composition, however, H-B humate contains magnesium and potassium. The amount of calcium and sodium is highest in both samples. In the sample H-B, the sodium content is higher, and the calcium content is lower than in the sample H-GK. The presence of calcium indicates the formation of the calcium phase, which is characterized as insoluble and less active. The calcium amount in H-GK humate is greater than in H-B humate, which may indicate its lower solubility. The presence of silicon and aluminum in both types of humates may indicate the formation of aluminosilicates. The most interesting results of elemental analysis are after the sorption of metal ions. After the sorption of heavy metals, both the number of the elements to be determined and their quantitative content are significantly reduced. This is especially true for the H-B sample in the sorption of Pb^{2+}. The content of copper and lead ions is two times higher in H-B humates than in H-GK humates. In addition, the amount of sorbed lead ions is two times higher than the amount of sorbed copper ions in both types of samples.

3.2. TG analysis

The thermal stability of H-GK and H-B samples was characterized by thermogravimetric analysis (TGA) as shown in Fig. 2. The weight loss during the thermal treatment was observed for both samples up to 650°C. The thermal degradation was divided in two stages. The first stage up to 200°C is characterized by the mass loss of 14.23% and 16.57% due to the evaporation of physically adsorbed water,

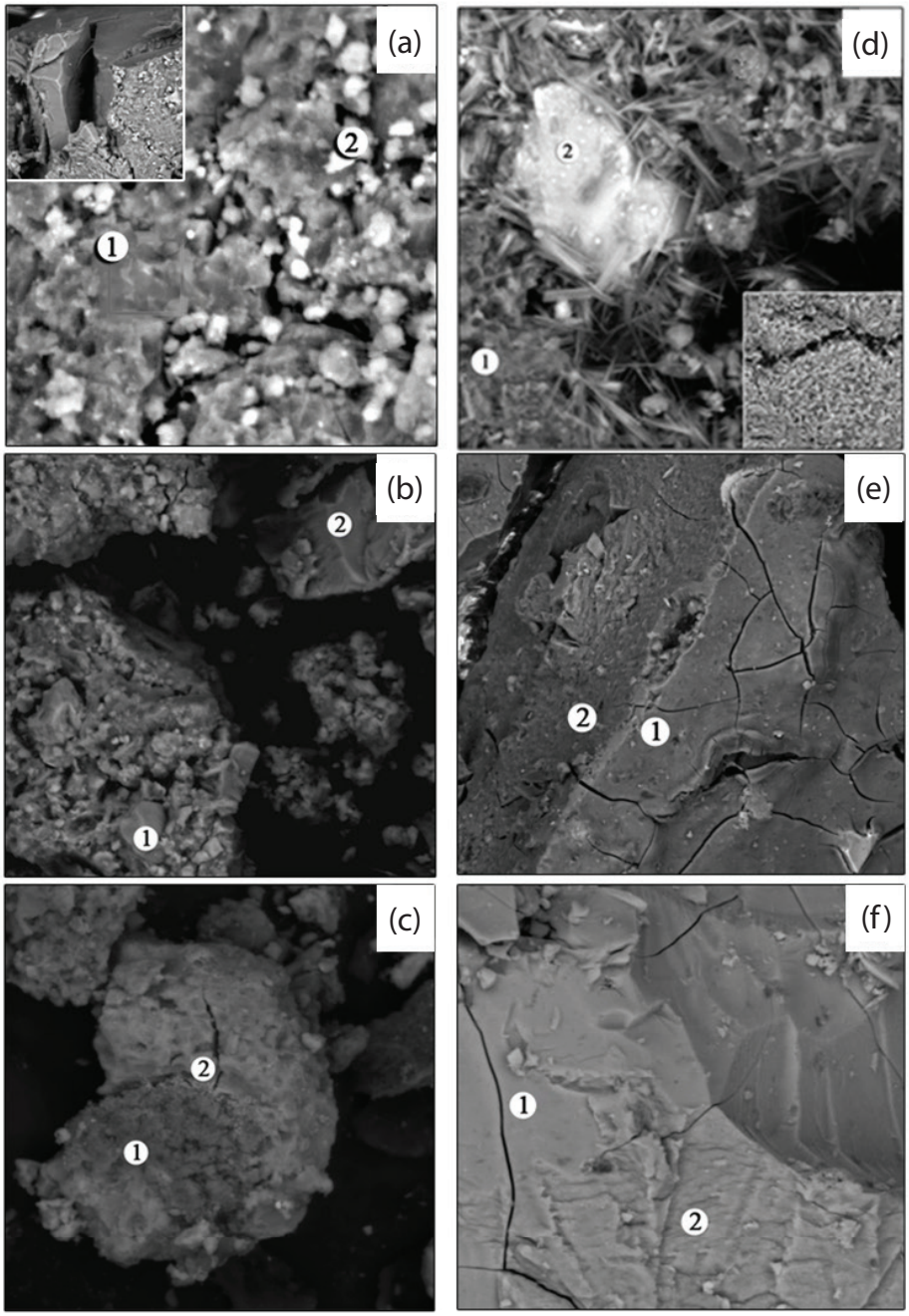

Fig. 1. SEM images of H-GK samples (a), H-GK+ Cu^{2+} (b), H-GK +Pb^{2+} (c) and H-B samples (d), H-B +Cu^{2+} (e), H-B + Pb^{2+} (f).

for H-GK and H-B samples respectively. After this common step, all samples showed a decomposition stage, in which the curves of both samples presented an abrupt organic mass loss being a lesser value of 21.59% for H-GK and a larger value of 25.85% for the H-B sample (Table 3).

3.3. IR-spectroscopy

To get information about functional groups of humates and their chemical behavior after the binding of metal ions, FTIR spectra were measured (Fig. 3).

The broad peaks at 3,300 and 3,370 cm^{-1} are attributed to the O–H stretching vibrations of aromatic and aliphatic groups as well as the peaks at 3,800 and 3,660 cm^{-1}. It means that the largest amounts of hydrating water are included in humates and humic hydro complexes of Cu^{2+} and Pb^{2+}.

A discrete peak at about 1,560 cm^{-1} (H-GK sample) and 1,550 cm^{-1} (B-H sample) are likely ascribed to aromatic C=C stretching. The peak shifting to 1,581 cm^{-1} is observed after Cu^{2+} ions are sorbed onto the surface of the H-B sample.

The characteristic peaks at about 1,378–1,369 cm^{-1} are associated to C–H deformation of CH_2 and CH_3 groups,

Table 1
Elemental composition of H-GK sample before and after sorption metal (Fig. 1(a)–(c))

Point	Elements content (wt%)									
	O	Na	Mg	Al	Si	Cl	S	Ca	Fe	Ions
Initial H-GK sample										
1	54.5	20.3	–	1.8	0.8	–	2.0	16.5	4.2	–
2	62.6	9.8	–	2.8	2.5	–	0.4	20.9	1.0	–
Range	54.5–62.6	6.7–24.4	0.0–1.2	0.8–7.6	0.0–7.4	–	0.3–2.0	7.8–20.9	0.9–4.2	–
H-GK sample+ Cu^{2+}										Cu
1	10.15	0.25	–	0.43	0.14	–	0.38	2.81	0.54	10.13
2	1.02	0.05	–	0.17	0.16	–	0.01	0.53	0.51	6.14
Range	1.02–29.29	0.05–0.52	–	0.17–0.46	0.14–0.24	–	0.01–0.46	0.53–3.05	0.00–0.54	6.14–10.36
H-GK sample+ Pb^{2+}										Pb
1	12.37	0.47	–	1.06	0.91	–	–	2.72	0.43	25.03
2	4.59	0.11	–	1.00	1.30	–	–	9.68	–	5.84
Range	4.59–29.71	0.11–2.50	0.00–0.24	0.25–2.94	0.10–2.73	0.09–0.41	–	1.03–9.68	0.00–0.57	1.73–28.59

Table 2
Elemental composition of H-B sample before and after sorption metal (Fig. 1(d)–(f))

Point	Elements content (wt%)										
	O	Na	Mg	Al	Si	Cl	K	S	Ca	Fe	Ions
Initial H-B sample											
1	48.8	46.8	–	1.0	1.2	–	–	0.5	1.5	0.2	–
2	44.8	9.0	5.8	9.0	14.1	–	4.6	0.1	0.4	10.6	–
Range	39.9–72.4	1.7–47.6	0.0–5.8	0.3–17.4	0.4–37.5	0.5–5.0	0.1–12.1	0.1–8.1	0.1–18.6	0.1–10.6	–
H-B sample+Cu^{2+}											Cu
1	17.04	1.78	–	0.99	0.90	0.28	–	1.28	0.17	0.28	11.80
2	3.04	0.35	–	0.35	0.16	0.03	–	0.12	0.03	0.21	8.44
Range	0.48–28.31	0.00–3.81	0.00–0.47	0.04–7.54	0.08–4.90	0.03–0.89	0.01–0.07	0.12–4.93	0.00–0.22	0.00–0.57	8.44–25.43
H-B sample+Pb^{2+}											Pb
1	16.52	0.28	–	0.15	0.13	–	–	–	–	–	36.02
2	16.86	0.24	–	0.24	–	–	–	–	0.28	–	35.61
Range	16.52–18.91	0.22–0.64	–	0.15–0.51	0.10–0.17	–	–	–	0.00–0.28	–	35.22–37.22

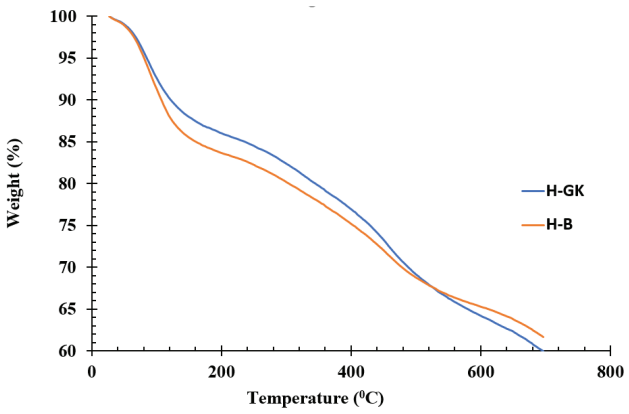

Fig. 2. TGA curves of humates.

and/or antisymmetric stretching of COO− groups shifting to 1,380 cm^{-1} after Cu^{2+} on H-B sample.

The noticeable peak at 2,019 cm^{-1} appears at the spectra both of H-B and H-GK samples after binding of Cu^{2+} ions. It attributes to the copper dycarbonyl ($Cu(CO)_2$) stretching vibrations of C–O bonds [41].

The reaction between the metal ion and COOH functional groups, forming a metal ion complex [42], results in the disappearance of the 989 cm^{-1} absorption band (H-B sample) and shifting in the frequencies of the absorption band from 1,020 to 1,036 (H-GK sample, Fig. 2).

According to FTIR experiments sorption of Cu^{2+} ions onto the surface of H-B and H-GK samples are assumed to occur through 1) the formation of copper dycarbonyl ($Cu(CO)_2$) and 2) ion-exchange mechanism involving carboxyl group [28]:

Table 3
Percentages of mass losses (Δ*m*) and the respective temperature range (*T*) for H-GK and H-B samples

Sample	Δ*m* (%)	*T*(°C)
H-B	14.23	≤180
	25.85	180–650
H-GK	16.57	≤180
	21.59	180–650

$$COOH \rightarrow COO^- + H^+ \quad (3)$$

$$COO^- + Cu^{2+} \rightarrow COO^- Cu^{2+} \quad (4)$$

In the case of lead sorption, the broad peaks at 3,419 and 3,383 cm^{-1} specific for H-GK sample+Pb^{2+} (Figs. 3(a), curve 3) and H-B sample+Pb^{2+} (Fig.2(b), curve 3) correspond to O–H stretching and N–H stretching of various functional groups [35]. For H-GK sample+Pb^{2+} are observed a group of peaks at 3,689 and 3,618 cm^{-1} is related to O–H stretching of hydroxyl groups [43].

The peaks at 2,850 and 2,922 cm^{-1} are attributed to the symmetric and asymmetric C–H stretching vibrations of aliphatic C–H bonds in CH_3 and CH_2 groups respectively [44].

At 1,377 and 1,373 cm^{-1} for H-GK sample+Pb^{2+} and H-B sample+Pb^{2+} are observed C–H deformation of CH_2 and CH_3 groups and stretching of COO− and CH_3 groups, and peaks at 1,566 and 1,558 cm^{-1} indicate the presence of COO− and C=O stretching [45].

For both samples after Pb^{2+} sorption (Figs. 2(a) and (b), curve 3) observed several bands related to Si–O stretching. The peaks at 788, 1,012, 1,034, 1,115 cm^{-1} for H-GK sample+Pb^{2+} and 779, 1,007 and 1,031 cm^{-1} for H-B sample+Pb^{2+} also spectra are characterized by the presence of Si–O–R (R = Al, Fe, Si) deformation at 472 cm^{-1}. Moreover, there are Al–O–Si deformation at 540 cm^{-1} and Si–O perpendicular at 752 cm^{-1} for H-GK sample+Pb^{2+}.

The peaks at 689 and 669 cm^{-1} for both samples point to OH bending, peaks at 914 and 938 cm^{-1} for H-GK sample+Pb^{2+} demonstrate OH deformation of hydroxyl groups.

IR spectra for the initial humate and after lead sorption have a similar type of functional groups, but a shift in the peaks and a change in their intensity are observed. Thus, a region of OH vibrations (3,419 and 3,383 cm^{-1}) and the COO– oscillation region (1,377, 1,566, 1,373, and 1,558 cm^{-1}) for humate after lead sorption shifted to the right relative initial humate and have a higher intensity. This indicates that the phenolic and carboxyl groups are involved in the sorption process [46].

3.4. Effects of contact time, pH, and a dose of humate

Metal ions have a high affinity for the functional groups present in humic substances, they could be effectively removed from the solutions.

The effects of contact time (0.5–4 h) on Cu^{2+} and Pb^{2+} removal efficiency were studied with an initial metal ion concentration of 300 mg L^{-1}. The initial pH values were 5.2 and 6.0 for Cu^{2+} and Pb^{2+} solutions, respectively. The pH of

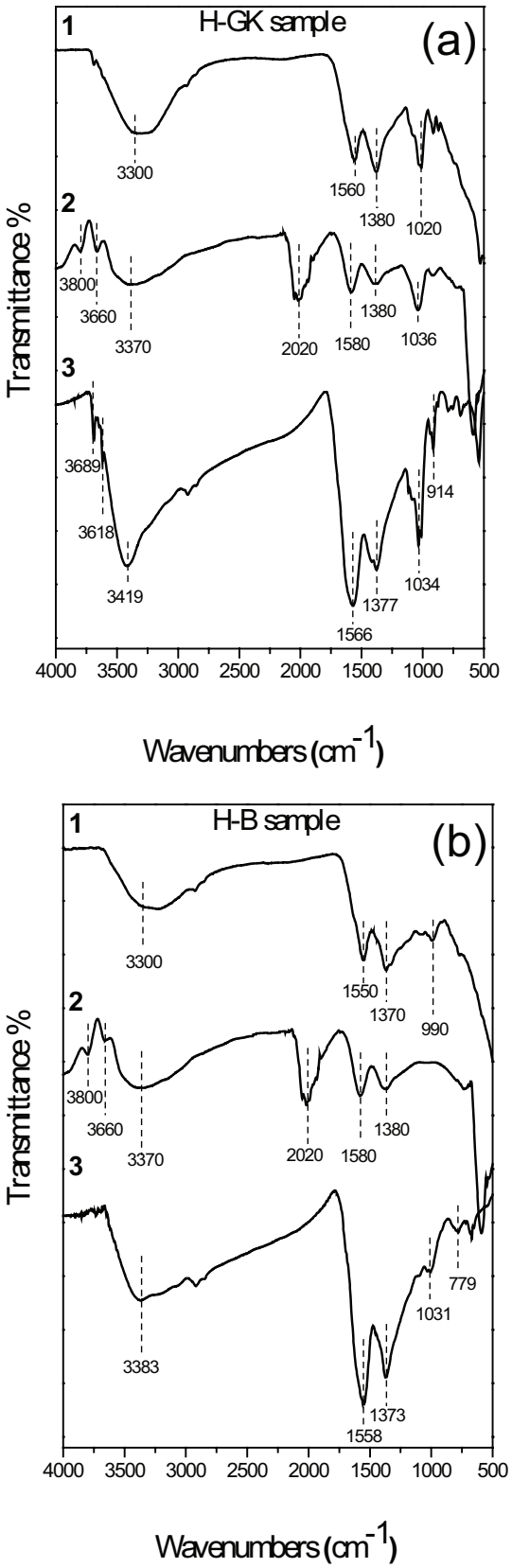

Fig. 3. FTIR-spectra of humates, (a) 1-H-GK sample, 2-H-GK sample+Cu^{2+}, 3-H-GK sample+Pb^{2+}; (b) 1-H-B sample, 2-H-B sample+Cu^{2+}, 3-H-B sample+Pb^{2+}.

the solutions treated with humates varied from 5.4 to 5.6 and from 6.2 to 7.2 for Cu^{2+} and Pb^{2+}solutions, respectively and depended on the humate dose.

Figs. 4 and 5 demonstrate the effects of contact time and a dose of humates on the removal efficiency of metal ions. It is obvious that the optimal contact time is 1 h and it doesn't depend on the type and dose of humate.

The removal efficiency of copper ions is lower than the removal efficiency of lead ions. Also, the effective removal (80%–81%) of lead ions is reached at smaller doses (600 mg L^{-1}), while copper removal efficiency of 54%–65% is reached only at 1,400 mg L^{-1} of H-B sample.

Comparison of sorption capacity of H-B and H-GK samples showed that H-GK binds metal ions worth than H-B and large doses of sorbent are needed. It can lead to the pollution of water with humic substances.

Also, the results show that both H-B and H-GK samples bind lead ions better than copper ones. It may be caused by the following reasons. The first is that the binding ability of ions strongly depends on the ion radius and charge density. If we compare two ions with the same charge greater adsorption capacity shows the ions of larger radius, as they are stronger and better polarized are attracted to the charged surface of the sorbent and the ions of the smaller radius are more likely to hydration and formation of hydration shells that reduce such electrostatic interaction. Since lead has a larger ionic radius (0.126 nm) in comparison with ions of copper (0.08 nm), the sorption capacity of sorbents in relation to lead ions should be higher than with respect to copper ions, which is confirmed by experimental data [47]. According to the principle of "Hard and Soft Acid and Base"(Pearson's rule) [48], the Pb^{2+} is classified in the borderline metal acids, while Cu^{2+} ion is classified as a soft metal acid, the greater stability of the Pb^{2+}-humate complex compared with the complexes with copper can be expected. So, Pb^{2+} was found to form the most stable complex with the oxygen-carrying donor groups of humic substances.

The binding of ions is affected by the stability constant. The bigger it is, the better the binding of the heavy metal ion. For lead ions, the stability constant is equal to 2.58; whereas for copper ions, it is 2.35 [31,38].

It is well known that the changes in pH values of an external solution can influence the sorption behavior of a metal ion by a binding agent. Fig. 5 performs the effect of humates dose on the removal efficiency of Cu^{2+} and Pb^{2+} ions at pH = 2.

It is apparent that the removal efficiency is low and only reaches 19%–20% for Cu^{2+} ions removed with a high dose of H-B sample (2,400 mg L^{-1}). Solution pH affects both humates surface metal binding sites and the metal chemistry in water. So, we reported a little metal binding ability at pH = 2. That is because the surface of the sorbent is closely associated with the hydronium ions and repulsive forces limit the approach of the metal ions.

When the pH value increases, more protons are greatly combined with OH– that is resulting in H_2O molecules

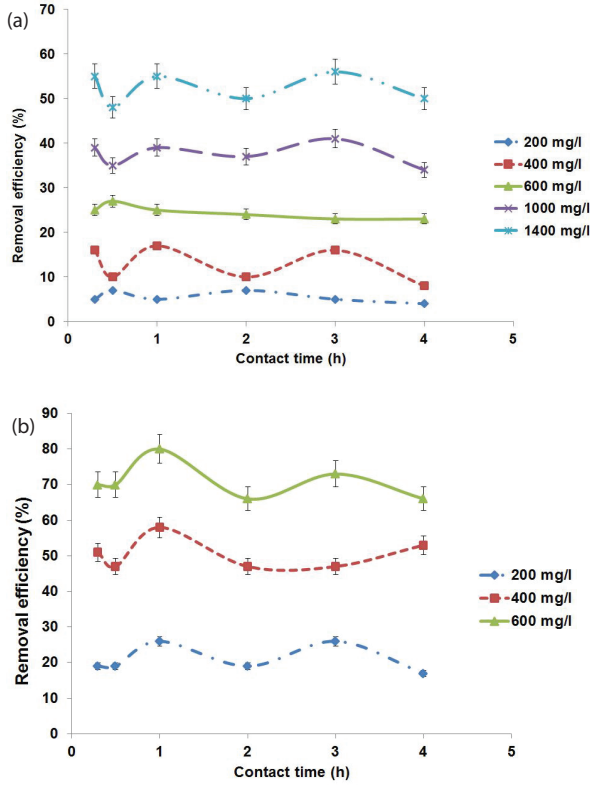

Fig. 4. Effect of contact time and a dose of humate on removal efficiency of metal ions with H-B samples: (a) Cu^{2+} ions; initial concentration is 300 mg L^{-1}; pH = 5.4–5.6, (b) Pb^{2+} ions; initial concentration is 300 mg L^{-1}; pH = 6.2.

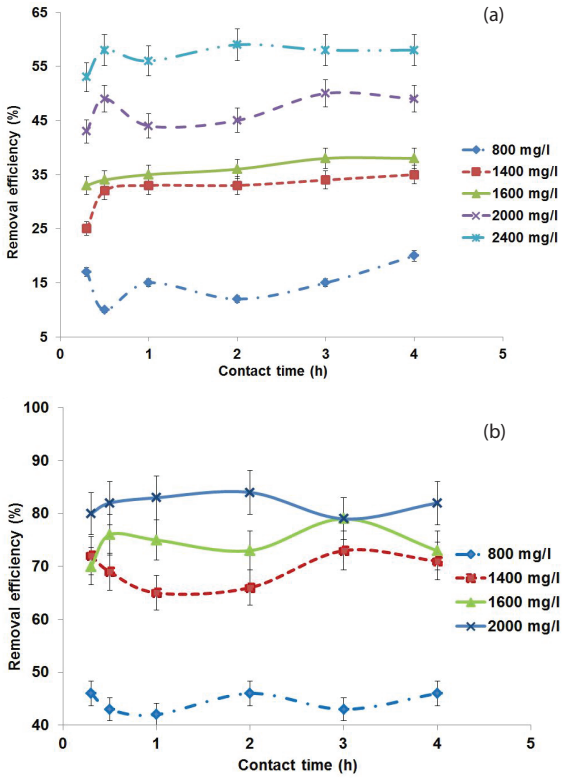

Fig. 5. Effect of contact time and dose of humate on removal efficiency of metal ions with H-GK samples: (a) Cu^{2+} ions; initial concentration is 300 mg L^{-1}; pH = 5.4–5.6, (b) Pb^{2+} ions; initial concentration is 300 mg L^{-1}; pH = 6.2–7.2.

production. In this case, Me^{2+} and $Me(OH)^{+}$ species are observed in the solution. The authors [49] reported a similar result for humate and copper(II) ions, suggesting that copper-humate complexes are not formed at pH = 2 because of strong competition of H^{+} for COOH binding sites. For both Cu^{2+} and Pb^{2+} ions the higher the pH, the greater will be the dissociation of the functional groups –COOH and –COH to –COO–and –CO–. For example, for Cu^{2+} solution treated by 1,400 mg L^{-1} dose of H-B sample, when the solution pH varied from 2.0 to 5.4 the removal efficiency increased from 18% to 54% (Figs. 4(a) and 6(a)). In the case of $Pb^{2+,}$ the removal efficiency increased from 6% to 45% when pH increased from 2 to 6.2 (Fig. 6(b) and 4(b)) for humate dose of 800 mg L^{-1}.

3.5. Effect of metal concentration

The amount of metal ion binding with the humates particles varies with the amount of taken humate and the concentration of the used metal salt solution. Earlier we set that binding of lead ions samples is going better than copper ions using smaller humates doses. So, the effect of metal concentration on removal efficiency was studied at H-B doses of 400 and 1,400 mg L^{-1} and at H-GK doses of 800 and 2,400 mg L^{-1} for Pb^{2+} and Cu^{2+} removal, respectively. The range of metal ions concentration varied from 300 to 900 mg L^{-1}.

Fig. 7 reveals a sharp decline in removal efficiency with increasing metal ions concentration. The removal efficiency

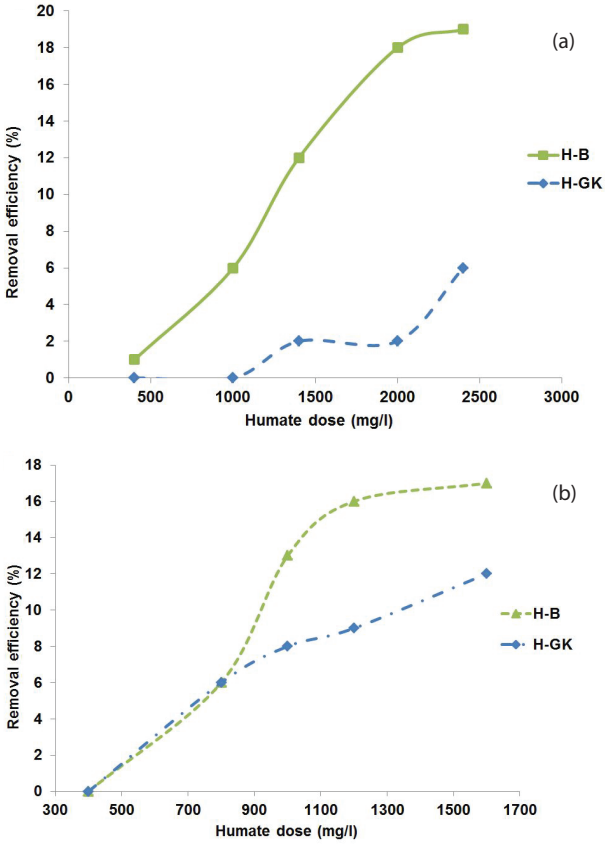

Fig. 6. Effect of humates dose on removal efficiency of Cu^{2+} (a) and Pb^{2+} (b) ions at pH = 2 (Initial metal ion concentration = 300 mg L^{-1}, contact time = 1h).

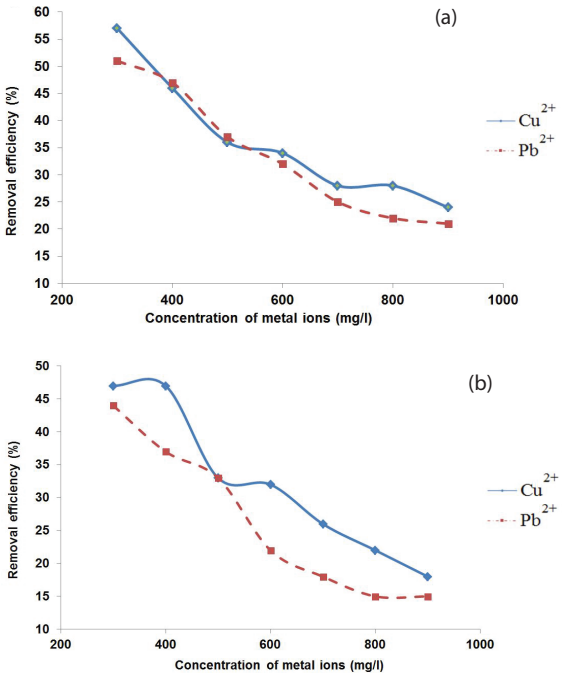

Fig. 7. Effect of metal concentration on removal efficiency of metal ions: (a) H-B sample (H-B doses are 400 and 1,400 mg L^{-1} for Pb^{2+} and Cu^{2+} removal, respectively; contact time = 1 h; pH = 5.4), (b) H-GK sample (H-GK doses are 800 and 2,400 mg L^{-1} for Pb^{2+} and Cu^{2+} removal, respectively; contact time = 1 h; pH = 6.2–7.2).

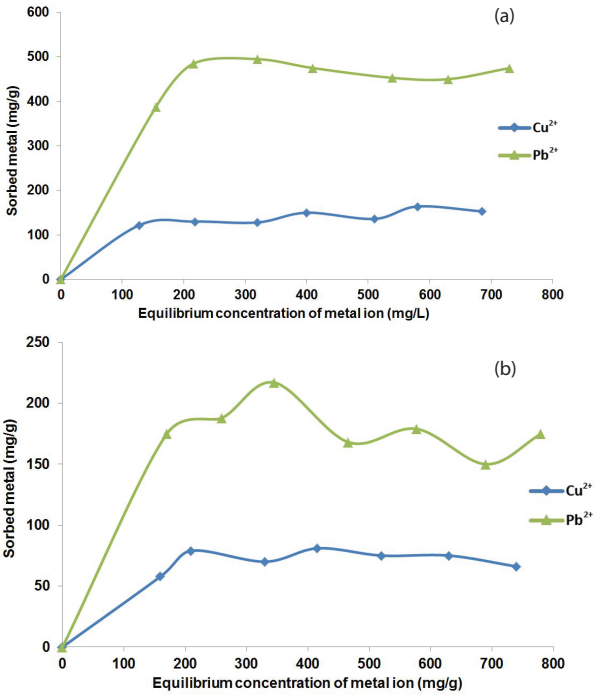

Fig. 8. Dependence of the amount of metal (in mg g^{-1} of humate sample) on equilibrium concentration of metal ion, (a) H-B (H-B doses are 400 and 1,400 mg L^{-1} for Pb^{2+} and Cu^{2+} removal, respectively; contact time = 1 h; pH = 5.4), (b) H-GK sample (H-GK doses are 800 and 2,400 mg L^{-1} for Pb^{2+} and Cu^{2+} removal, respectively; contact time = 1 h; pH = 6.2–7.2).

of $Pb^{2+}$with the increase in its concentration from 300 to 900 mg L^{-1} decreased from 52% to 22%, 44% to 15% for H-B and H-GK sorbents, respectively. The removal percentage of Cu^{2+} with the increase in its concentration from 300 to 900 mg L^{-1} decreased from 56% to 25%, 47% to 17% for H-B and H-GK sorbents, respectively. These results indicate that the initial metal ions concentration plays an important role in the sorption onto the humates surface.

H-B samples revealed the sorption capacity of 122 and 388 mg g^{-1} and H-GK samples of 58 and 350 mg g^{-1} for Cu^{2+} and Pb^{2+} ions, respectively, which is no worse than already studied humates (Table 4). For example, the authors [50] revealed the sorption capacity of sodium humates to Cu^{2+} as 50 mg g^{-1}. Zheng Y [28] reported low sorption capacity (14 mg g^{-1}) of insolubilized humic acid used for removal of Pb^{2+} ions (initial concentration 400 mg L^{-1}). Havelcova M. [51], showed the comparative results of Cu^{2+} and Pb^{2+} sorption capacities onto lignite and solid humic substances derived from it (130–190 mg g^{-1} and 40–120 mg g^{-1} for Pb^{2+} and Cu $^{2+}$ ions, respectively).

3.6. Desorption studies

To study the possibility to recover the humate-based sorbents, the desorption experiments were performed. Three different acids (HCl, HNO_3, and H_2SO_4) were used.

It was observed that all three acids are good eluents for H-B and H-GK regeneration. As we can see, in most cases, desorption reaches 100%. The elution of Cu^{2+} ions from the H-B sample by HCl, HNO_3, and H_2SO_4 was maximum and reached 100%. Sulfuric acid showed the worst result in lead elution from both H-B (26%) and H-GK (19%) samples (Fig. 9). It may be due to the low reactive activity of sulfuric acid with respect to the bonds of the lead with phenolic and carboxyl groups of humates.

3.7. Kinetic study

To analyze the sorption rate of Cu^{2+} and Pb^{2+} ions on H-B and H-GK samples during, a pseudo-second-order rate equation was used to simulate the kinetic sorption [59].

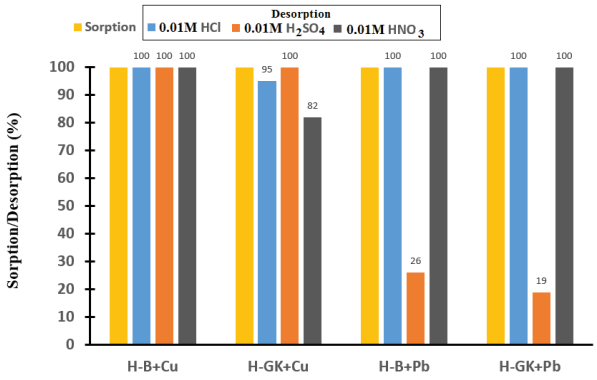

Fig. 9. Desorption plots of Cu^{2+} and Pb^{2+} from H-B and H-GK samples by different eluents.

Table 4
Comparison of Pb^{2+} and Cu^{2+} maximum sorption capacities on different carbon-based sorbents

Type of sorbent	Metal	Maximum sorption capacity	Temperature (C°)	pH	Reaction time (min)	Reference
Schiff base ligand based nano-composite adsorbent	Cu(II)	173.62 mg g^{-1}	Room temperature	7	120	[52]
Activated carbons using Fig sawdust by chemical activation with H_3PO_4	Pb(II)	80.645 mg g^{-1}	60	4	50	[53]
Ash	Pb(II)	588.24 mg g^{-1}	25	6	40	[53]
nFe-A	Pb(II)	833.33 mg g^{-1}	25	6	40	[53]
MWCNTs/ThO_2 nanocomposite	Pb(II)		45	5,5	50	[54]
Nano-composite cation exchanger sodium dodecyl sulfate acrylamide Zr(IV) selenite	Pb(II)	21.01 mg g^{-1}	55	6	40	[55]
T(IV) iodovanadate cation exchanger	Pb(II)	63.29 mg g^{-1}	45	6	60	[56]
Lignitic Humic Acids	Cu(II)	–	25		1,440 (24 h)	[57]
Lignite and humic acid	Pb(II)	2.32 mmol g^{-1} (480 mg g^{-1})	25	6	1,440 (24 h)	[51]
Lignite and humic acid	Cu(II)	1.49 mmol g^{-1} (95 mg g^{-1})	25	6	1,440 (24 h)	[51]
Iron humate	Cu(II)	0.109 mmol g^{-1} (7 mg g^{-1})	22	3–5	4,320 (72 h)	[58]
H-B	Cu(II)	122 mg g^{-1}	20	5.2–5.4	60	Present study
	Pb(II)	388 mg g^{-1}				
H-GK	Cu(II)	58 mg g^{-1}		6.2–7.2		
	Pb(II)	350 mg g^{-1}				

$$t/q_t = 1/\left(K_2 \cdot q_e^2\right) + t/q_e \quad (5)$$

where K_2 (g/mg*h) is the pseudo-second-order rate constant of sorption, q_t (mg g^{-1} of dry weight) is the amount of Cu^{2+}/Pb^{2+} sorbed on H-B and H-GK samples at time t (h), and q_e (mg g^{-1} of dry weight) is the equilibrium sorption capacity.

The plots of t/q_t vs. t at different temperatures (Fig. 10) showed good linearity; implying that the sorption system studied follows the pseudo-second-order kinetic model. The K_2 and q_e values calculated from the slope and intercept are presented in Table 5. The low values of K_2 suggested that the sorption of Cu^{2+} and Pb^{2+} achieved equilibrium quickly, whereas the values of q_e were quite close to the maximum data shown in Fig. 8. The correlation coefficients (R^2) for the linear plots were very close to 1, which suggested that the kinetic sorption could be described by a pseudo-second-order rate equation well. It means that the rate-limiting step may be chemical sorption involving valency forces through sharing or the exchange of electrons between the sorbent and the metal ions [60].

3.8. Thermodynamic study

Sorption of Cu^{2+} and Pb^{2+} on H-B and H-GK samples at different temperatures were carried out to study the influence of temperature on metal ion sorption and to achieve the thermodynamic data. The values of enthalpy, $\Delta H°$, and entropy, $\Delta S°$, were calculated from the slope and intercept of the plot of ln K_d vs. $1/T$ (Fig. 11) by using the equation:

$$\mathrm{Ln}K_d = \frac{\Delta S°}{R} - \Delta H°/RT \quad (6)$$

where R (8.3145 J mol K^{-1}) is the ideal gas constant, T (K) is the temperature.

The distribution coefficient (K_d) was calculated according to the following equation:

$$K_d = \frac{C_0 - C_e}{C_e} \times \frac{V}{m} \quad (7)$$

where C_0 is initial metal ion concentration (mg L^{-1}); C_e is the equilibrium metal ion concentration (mg L^{-1}), V is the volume of the solution (L) and m is the mass of the sorbent (g).

The Gibbs free energy, $\Delta G°$, was calculated from the equation:

$$\Delta G° = \Delta H° - T\Delta S° \quad (8)$$

The plots of ln K_d vs. $1/T$ were found to be linear with R^2 values greater than 0.9975. The $\Delta H°$ values ranged from 4 to 10.6 kJ mol^{-1} and from –7.5 to –12.5 kJ mol^{-1} for H-B and H-GK samples, respectively (Table 6).

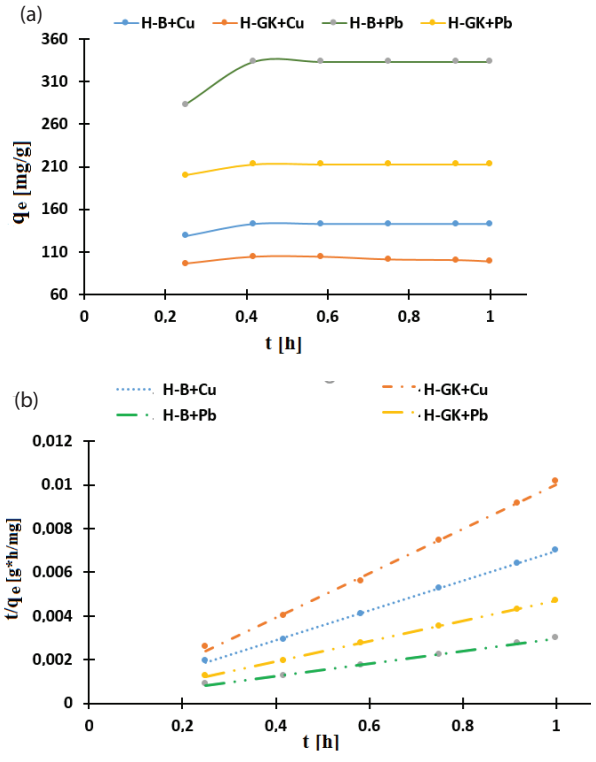

Fig. 10. Sorption of Pb^{2+} and Cu^{2+} as a function of contact time (a) and the pseudo-second-order kinetic of Pb^{2+} and Cu^{2+} sorption (b) on H-B and H-GK samples.
Note: C[Cu^{2+}/Pb^{2+})] initial = 300 mg L^{-1}, pH (H-B+Cu) = pH (H-B+Pb) = 5.4, pH (H-GK+Cu) = pH (H-GK+Pb) = 6.2, m(H-B) /V(Cu^{2+}) = 1,400 g L^{-1}, m(H-B) /V(Pb^{2+}) = 300 mg L^{-1}, m(H-GK) /V(Cu^{2+})= 2,400 g L^{-1}, m(H-GK) /V(Pb^{2+}) = 1,000 mg L^{-1}, T = 20°C.

Table 5
Fitted pseudo-second-order-model kinetic parameters for the removal of Cu^{2+}/Pb^{2+} ions by H-GK and H-B samples

Sample	K_2 (g/mg*h)	q_e (mg g^{-1})	R^2
H-GK+Cu	1.040	98	0.9975
H-B+Cu	0.231	147	0.9991
H-GK+Pb	0.352	217	0.9997
H-B+Pb	0.084	344	0.9977

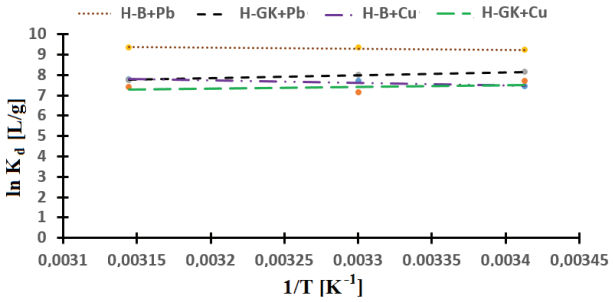

Fig. 11. Effect of temperature on the distribution coefficients of Cu^{2+} and Pb^{2+} on H-B and H-GK samples.
Note: C[Cu^{2+}/Pb^{2+})] initial = 300 mg L^{-1}, pH (H-B+Cu) = pH (H-B+Pb) = 5.4, pH (H-GK+Cu) = pH (H-GK+Pb) = 6.2, m(H-B) /V(Cu^{2+}) = 1,400 g L^{-1}, m(H-B) /V(Pb^{2+}) = 300 mg L^{-1}, m(H-GK) /V(Cu^{2+}) = 2400 g L^{-1}, m(H-GK) /V(Pb^{2+}) = 100 mg L^{-1}.

Table 6
Thermodynamic values of Cu^{2+} and Pb^{2+} sorption on H-B and H-GK samples

Sample	$\Delta H°$ (kJ mol^{-1})	$\Delta S°$ (J mol^{-1})	$\Delta G°$ (kJ mol^{-1})		
			293 K	303 K	318 K
H-B+Cu	10.6	98.3	–18.2	–29.7	–20.7
H-GK+Cu	–7.5	36.8	–18.3	–11.1	–19.2
H-GK+Pb	–12.5	24.9	–19.9	–7.5	–20.5
H-B+Pb	4.0	90.6	–22.5	–27.4	–24.8

It is evident from Table 6 that the values of $\Delta H°$ are positive (endothermic sorption) and negative (exothermic) for sorption on H-B and H-GK samples, respectively. The sorption is a multistep process. As a result of this process, the enthalpy of the sorption process of hydrated Cu^{2+} and Pb^{2+} ions is determined by the enthalpy of complex formation with functional groups and the system's energy costs associated with the dehydration of metal cations and functional ion exchanger groups.

The complex formation is the exothermic process while dehydration of ions and the change of polymer conformations chains in humates are endothermic. So, in the case of the H-GK sample, complex formation is a dominant process.

The values of $\Delta G°$ were negative at all temperatures that confirmed the feasibility of the sorption process. The positive value of $\Delta S°$ indicates that ion exchange reactions occurred [61].

So, we propose the following sorption mechanism. Two parallel processes occur (1) dehydration of metal cations, and (2) metal-humate complex formation as a result of ion exchange reactions. The phenolic and carboxyl groups of humates are involved in the sorption process.

4. Conclusions

In this study, two commercial samples of humates obtained from brown coal wastes used to investigate sorption ability to Cu^{2+} and Pb^{2+} from highly concentrated aqueous solutions. The morphology, elemental composition, and structure of soluble (H-B) and insoluble (H-GK) humates in combination with their sorption properties were investigated in order to clarify the mechanisms of sorption. The SEM and microelement analysis of various humate regions showed a multiphase structure in both pristine H-GK and H-B humate samples, which changes significantly as a result of the sorption of heavy metals. It is observed that copper and lead are built in different ways into the humic matrix: copper forms aggregates in the structure of humates while lead is scattered in a humid matrix with forming of films, relatively lead-enriched. This indicates the existence of various sorption mechanisms. In confirmation of this, the analysis of FTIR spectra revealed that sorption of Cu^{2+} ions of H-B and H-GK samples is assumed to occur through formation of copper dycarbonyl ($Cu(CO)_2$) and ion-exchange mechanism. At the same time, in the case of lead sorption, it was shown that the phenolic and carboxyl groups are involved in the sorption process.

Comparison of sorption capacity of H-B and H-GK samples showed that H-GK binds metal ions worth than H-B and large doses of sorbent are needed, as evidenced by the data of EDX analysis. Both the structure and the elemental composition may be the cause of such properties. Also, both H-B and H-GK samples bind lead ions better than copper ions due to the fact that the binding ability of ions strongly depends on the ion radius and charge density, that also in good agreement with elemental analysis.

The experimental results indicate that efficient removal of heavy metals occurs at pH = 5.4–5.6 and 6.2–7.2 for Cu^{2+} and Pb^{2+} solutions, respectively. The optimal contact time was certified to be as 1 h for both types of humate samples.

It was observed that HCl, HNO_3, H_2SO_4 acids are good eluents for H-B and H-GK regeneration (desorption reaches 100%). The sorption process was kinetically studied by fitting the experimental data with pseudo second order kinetic model and the results designated that the sorption followed it well.Thermodynamic studies showed that the values of $\Delta G°$ were negative at all temperatures confirming the feasibility of the sorption process. The positive value of $\Delta S°$ indicated that ion exchange reactions occurred.

Acknowledgments

The research is supported by the Southern Federal University Development Program. We thank the professor G.Yalovega for valuable discussion and help in interpreting the results, LLC "Agrarniye technologii" (Irkutsk, Russia) for humate samples.

References

[1] N.T. Abdel-Ghani, G.A. El-Chaghaby, Biosorption for metal ions removal from aqueous solutions: a review of recent studies, Int. J. Latest Res. Sci. Technol., 3 (2014) 24–42.
[2] G. Gyananat, D.K. Balhal, Removal of lead (II) from aqueous solutions by adsorption onto chitosan beads, Cellul. Chem. Technol., 46 (2012) 121–124.
[3] Taubayeva A.S. Development of technology for obtaining sorbents based on humic substances, Of the dissertation for Doctor of Philosophy (PhD) degree 6D072000 - Chemical technology of inorganic substances, 2014.
[4] T.J.K. Ideriah, S. David-Omiema, D.N. Ogbonna, Distribution of heavy metals in water and sediment along Abonnema Shoreline, Nigeria, Res. Environ., 2 (2012) 33–40.
[5] C. Elicker, P.J. Sanches Filho, K.R.L. Castagno, Electroremediation of heavy metals in sewage sludge, Braz. J. Chem. Eng., 31 (2014) 365–371.
[6] Y. Cao, X. Qian, Y. Zhang, G. Qu, T. Xia, X. Guo, H. Jia, T. Wang, Decomplexation of EDTA-chelated copper and removal of copper ions by non-thermal plasma oxidation/alkaline precipitation, Chem. Eng. J., 362 (2019) 487–496.
[7] H. Bai, S. Wei, Z. Jiang, M. He, B. Ye, G. Liu, Pb (II) bioavailability to algae (Chlorella pyrenoidosa) in relation to its complexation with humic acids of different molecular weight, Ecotoxicol. Environ. Saf., 167 (2019) 1–9.
[8] S. Thaçi Bashkim, T. Gashi Salih, Reverse osmosis removal of heavy metals from wastewater effluents using biowaste materials pretreatment, Pol. J. Environ. Stud., 28 (2019) 337–341.
[9] J. López, M. Reig, O. Gibert, J.L. Cortina, Recovery of sulphuric acid and added value metals (Zn, Cu and rare earths) from acidic mine waters using nanofiltration membranes, Separ. Purif. Technol., 212 (2018) 180–190.
[10] G.M. Kirkelund, P.E. Jensen, L.M. Ottosen, K.B. Pedersen, Comparison of two- and three-compartment cells for

electrodialytic removal of heavy metals from contaminated material suspensions, J. Hazard. Mater., 367 (2018) 68–76.
[11] A. Ishfaq, S. Ilyas, A. Yaseen, M. Farhan, Hydrometallurgical valorization of chromium, iron, and zinc from an electroplating effluent, Separ. Purif. Technol., 209 (2019) 964–971.
[12] A.A. Alqadami, M. Naushad, M.A. Abdalla, T. Ahamad, Z. Abdullah Alothman, S.M. Alshehri, Synthesis and characterization of Fe_3O_4@TSCnanocomposite: highly efficient removal of toxic metal ions from aqueous medium, RSC Adv., 6 (2016) 1–37.
[13] A.A. Alqadami, M. Naushad, M.A. Abdalla, T. Ahamad, Z. Abdullah ALOthman, S.M. Alsehri, A.A. Ghfar, Efficient removal of toxic metal ions from wastewater using a recyclable nanocomposite: a study of adsorption parameters and interaction mechanism, J. Cleaner Prod. 156 (2017) 426–436.
[14] A. Aldawsari, M.A. Khan, B.H. Hameed, A.A. Alqadami, M.R. Siddiqui, Z.A. Alothman, A.Y.B.H. Ahmed, Mercerized mesoporous date pit activated carbon — A novel adsorbent to sequester potentially toxic divalent heavy metals from water, PLOS ONE, 12 (2017) 1–17.
[15] M.A. Khan, A. Alqadami, M. Otero, M.R. Siddiqui, Z.A. Alothman, I. Alsohaimi, M. Rafatullah, A.E. Hamedelniel, Heteroatom-doped magnetic hydrochar to remove post-transition and transition metals from water: Synthesis, characterization, and adsorption studies, Chemosphere, 218 (2019) 1089–1099.
[16] S. Wua, J. Hu, L. Wei, Y. Dub, X. Shi, H. Deng, L. Zhang, Construction of porous chitosan–xylan–TiO_2 hybrid with highly efficient sorption capability on heavy metals, J. Environ. Chem. Eng., 2 (2014) 1568–1577.
[17] F. Fu, Q. Wang, Removal of heavy metal ions from wastewaters: a review, J. Environ. Manage., 92 (2011) 407–418.
[18] M. Klučáková, M. Pavlíková, Lignitic humic acids as environmentally-friendly adsorbent for heavy metals, J. Chem., (2017) 1–5.
[19] E. Lipczynska-Kochany, Humic substances, their microbial interactions and effects on biological transformations of organic pollutants in water and soil: a review, Chemosphere, 202 (2018) 420–437.
[20] E.M. Osnitsky, M.P. Sartakov, E.A. Zarov, Y.M. Deryabina, Elemental composition of the humic acids in the high-moor peats of the Western Siberia Taiga zone, Res. J. Pharm. Biol. Chem. Sci., 7 (2016) 3104–3113.
[21] W.M. Swiech, I. Hamerton, H. Zeng, D.J. Watson, E. Mason, S.E. Taylor, Water-based fractionation of a commercial humic acid. Solid-state and colloidal characterization of the solubility fractions, J. Colloid Interface Sci., 508 (2017) 28–38.
[22] T. Skripkina, A. Bychkov, V. Tikhova, B. Smolyakov, O. Lomovsky, Mechanochemically oxidized brown coal and the effect of its application in polluted water, Environ. Technol. Innovation, 11 (2018) 74–82.
[23] V.A. Rumyantsev, A.S. Mityukov, L.N. Kryukov, G.S. Yaroshevich, Unique properties of humic substances from sapropel, Dokl. Earth Sci., 473 (2017) 482–484.
[24] D. Kulikowska, Z.M. Gusiatin, K. Bułkowska, B. Klik, Feasibility of using humic substances from compost to remove heavy metals (Cd, Cu, Ni, Pb, Zn) from contaminated soil aged for different periods of time, J. Hazard. Mater., 300 (2015) 882–891.
[25] D. Jones, J. Mishler, Humate remediation petroleum contaminated shorelines. Turning ideas into action: ensuring effective clean up and restoration in the Gulf, Senate committee on commerce, science, and transportation, 111 congress USA, (2010) 29–37.
[26] M. Karr, Using Humic Substances in the Bioremediation of Petroleum Polluted Soils., (2018).
[27] M. Ma, Y. Wei, G. Zhao, F. Liu, Y. Zhu, Characterization and adsorption mechanism of Pb(II) removal by insolubilized humic acid in polluted water, Int. J. Environ. Protec. Policy, 2 (2014) 230–235.
[28] Y. Zheng, S. Hua, A. Wang, Adsorption behavior of Cu^{2+} from aqueous solutions onto starch-g-poly (acrylic acid)/sodium humate hydrogels, Desalination, 263 (2010) 170–175.
[29] S.M. Shaheen, F.I. Eissa, K.M. Ghanem, H.M. Gamal El-Din, F.S. Al Anany, Heavy metals removal from aqueous solutions and wastewaters by using various byproducts, J. Environ. Manage., 128 (2013) 514–521.
[30] P. Janos, M. Kormunda, F. Novak, O. Zivotsky, J. Fuitova, V. Pilarova, Multifunctional humate-based magnetic sorbent: preparation, properties and sorption of Cu(II), phosphates and selected pesticides, React. Funct. Polym., 73 (2013) 46–52.
[31] S. Ivana, Comparative study of binding strengths of heavy metals with humic acid, Hem. Ind., 67 (2013) 773–779.
[32] M. Klucakova, Comparative Study of binding behaviour of Cu(II) with humic acid and simple organic compounds by ultrasound spectrometry, Open Colloid Sci. J., 5 (2012) 5–12.
[33] I. Kostic, T. Anđelkovic, R. Nikolic, A. Bojic, M. Purenovic, S. Blagojevic, D. Anđelkovic, Copper(II) and lead(II) complexation by humic acid and humic-like ligands, J. Serb. Chem. Soc., 76 (2011) 1325–1336.
[34] D. Dudare, M. Klavins, The interaction between humic substances and metals, depending on structure and properties of humic substances. 4th International Conference on Environmental, Energy and Biotechnology, 85 (2015) 10–15.
[35] S. Erdogan, A. Baysal, O. Akba, C. Hamamci, Interaction of metals with humic acid isolated from oxidized coal, Poli. J. of Environ. Stud., 5 (2007) 671–675.
[36] L.V. Bryukhovetskaya, S.I. Zherebtsov, N.V. Malyshenko, Z.R. Ismagilov, Sorption of copper cations by native and modified humic acids., Coks. Chim., 59 (2016) 420–423.
[37] S.I. Zherebtsov, N.V. Malyshenko, L.V. Bryukhovetskaya, Z.R. Ismagilov, Interaction of copper, zinc, and manganese cations with lignite and humic acids, Coks. Chim., 60 (2017) 397–403.
[38] M. Levine Effect of pH on New Mex Humate Treatment, 2012.
[39] R. Vidali, E. Remoundaki, M. Tsezos, An experimental and modelling study of Cu^{2+} binding on humic acids at various solution conditions. Application of the NICA-Donnan model, Water Air Soil Pollut., 218 (2011) 487–497.
[40] A.I. Chechevatov, Y.S. Miroshnichenko, T.N. Myasoyedova, Y.V. Popov, G.E. Yalovega, Investigations of the capability to heavy metals adsorption humic acids: correlation between structure and absorption properties, Springer Proc. Physics., 193 (2017) 99–110.
[41] R.D. Pike, Structure and bonding in copper(I) carbonyl and cyanide complexes, Organometallics, 31 (22) (2012) 7647–7660.
[42] S.F. Lim, Y.M. Gzheng, S. Wenzou, J.P. Chen, Characterization of copper adsorption onto an alginate encapsulated magnetic sorbent by a combined FT-IR, XPS, and mathematical modeling Study, Environ. Sci. Technol., 42 (2008) 2551–2556.
[43] S.J. Parikh, K.W. Goyne, A.J. Margenot, F.N.D. Mukom, F.J. Calderón, Soil chemical insights provided through vibrational spectroscopy, Adv. Agron, 126 (2014) 1–148.
[44] V. Enev, L. Pospíšilová, M. Klučáková, T. Liptaj, L. Doskočil, Spectral characterization of selected humic substances, Soil Water Res., 9 (2014) 9–17.
[45] S. Orsetti, M. de las Mercedes Quiroga, E.M. Andrade, Binding of Pb(II) in the system humic acid/goethite at acidic pH, Chemosphere, 65 (2006) 2313–2321.
[46] W. Shi, C. Lü, J. He, H. En, M. Gao, B. Zhao, B. Zhou, H. Zhou, H. Liu, Y. Zhang, Nature differences of humic acids fractions induced by extracted sequence as explanatory factors for binding characteristics of heavy metals, Ecotoxicol. Environ. Saf., 154 (2018) 59–68.
[47] T. Bohli, I. Villaescusa, A.J. Ouederni, Comparative study of bivalent cationic metals adsorption Pb(II), Cd(II), Ni(II) and Cu(II) on olive stones chemically activated carbon, Chem. Eng. Process Technol., 4 (2013) 1–7.
[48] A. Alfarraa, E. Frackowiakb, F. Beguin, The HSAB concept as a mean to interpret the adsorption of metal ions onto activated carbons, Appl. Surf. Sci., 228 (2004) 84–92.
[49] J. Wu, L.J. West, D.I. Stewart, Effect of humic substances on Cu(II) solubility in kaolin-sand soil, J. Hazard Mater., 94 (2002) 223–238.
[50] J. Kochany, W. Smith, Application of humic substances in environmental remediation, In Proc. Humic Substances Seminar IV, (2001) 32.
[51] M. Havelcova, J. Mizera, I. Sykorova, M. Pekar, Sorption of metal ions on lignite and the derived humic substances, J. Hazard. Mater., 161 (2009) 559–564.

[52] Md. Rabiul Awual, G.E. Eldesoky, T. Yaita, Mu. Naushad, H. Shiwaku, Z.A. AlOthman, S. Suzuki, Schiff based ligand containing nano-composite adsorbent for optical copper(II) ions removal from aqueous solutions, Chem. Eng. J. 279 (2015) 639–647.
[53] M. Ghasemi, Mu. Naushad, N. Ghasemi, Y. Khosravi-fard, A novel agricultural waste based adsorbent for the removal of Pb(II) from aqueous solution: Kinetics, equilibrium and thermodynamic studies, J. Ind. Eng. Chem., 20 (2014) 454–461.
[54] A. Mittal, M. Naushad, G. Sharma, Z.A. Alothman, S.M. Wabaidur, M. Alam, Fabrication of MWCNTs/ThO_2 nanocomposite and its adsorption behavior for the removal of Pb(II) metal from aqueous medium, Desal. Wat. Treat., 57 (2016) 21863–21869.
[55] M. Naushad, Surfactant assisted nano-composite cation exchanger: development, characterization and applications for the removal of toxic Pb^{2+} from aqueous medium, Chem. Eng. J., 235 (2014) 100–108.
[56] M. Naushad, Z.A. ALOthman, Md. Rabiul Awual, M. Mezbaul Alam, G.E. Eldesoky, Adsorption kinetics, isotherms, and thermodynamic studies for the adsorption of Pb^{2+} and Hg^{2+} metal ions from aqueous medium using Ti(IV) iodovanadate cation exchanger, Springer-Verlag Berlin Heidelberg, 21 (2015) 2237–2245.
[57] M. KluIáková1, M. Pavlíková, Lignitic humic acids as environmentally-friendly adsorbent for heavy metals, J. Chem. 2017 (2017) 1–5.
[58] P. Janos, J. Fedorovic, P. Stanková, S. Grötschelová, J. Rejnek, P. Stopka, Iron humate as a low-cost sorbent for metal ions, Environ. Technol., 27 (2006) 169–181.
[59] D. Robati, Pseudo-second-order kinetic equations for modeling adsorption systems for removal of lead ions using multi-walled carbon nanotube, J. Nanostruct. Chem., 3 (2013) 49–55.
[60] Z. Aly, A. Graulet, N. Scales, T. Hanley, Removal of aluminium from aqueous solutions using PAN-based adsorbents: characterisation, kinetics, equilibrium and thermodynamic studies, Environ Sci. Pollut. Res., 21 (2014) 3972–3986.
[61] Y. Liu, Y.-J. Liu, Biosorption isotherms, kinetics and thermodynamics, Separ. Purif. Technol., 61 (2008) 229–242.